0026-895X/94/010151-10$03.00/0

MOLECULAR PHARMACOLOGY, 46:151-160, 1994.

9-Aminoacridines Act at a Site Different from that for Mg^{2+} in Blockade of the *N*-Methyl-D-Aspartate Receptor Channel

MARK E. NELSON and EDSON X. ALBUQUERQUE

Department of Pharmacology and Experimental Therapeutics, University of Maryland, School of Medicine, Baltimore, Maryland 21201, and Laboratório de Farmacologia Molecular II, Instituto de Biofísica Carlos Chagas Filho, Universidade Federal do Rio de Janeiro, Rio de Janeiro, CEP 21941, Brazil

Received February 14, 1994; Accepted April 26, 1994

SUMMARY

The effects of alkylene bis-9,9′-aminoacridines and 1,2,3,4-tetrahydro-9-aminoacridine (THA) were studied on single-channel currents activated by *N*-methyl-D-aspartate (NMDA) in outside-out patches from cultured rat hippocampal neurons. These compounds reduced the channel open times with concentration and voltage dependence, which was consistent with an open-channel blockade mechanism of action. In nominally Mg^{2+}-free solutions, the forward blocking rate constants for 1,2-propane-bis-9,9′-aminoacridine, 1,4-butane-9,9′-aminoacridine, and THA were 1.1×10^8, 1.4×10^8, and 3.5×10^7 M^{-1} sec^{-1}, respectively, at a holding potential of −80 mV. The unblocking rate constants for the bis-9-aminoacridines were similar and in the range of 7 sec^{-1}, whereas THA had an unblocking rate constant of approximately 6.2×10^3 sec^{-1}. In the presence of Mg^{2+} (~5 μM), the predictions of the model for open-channel blockade by the 9-aminoacridines were invalid, because the relationships between the channel lifetimes and 9-aminoacridine concentrations were not linear. The effects of Mg^{2+} (~0–50 μM) on the open-channel blockade of the NMDA receptor by the 9-aminoacridines were evaluated further by measuring the burst times in the presence of 1,2-propane-bis-9,9′-aminoacridine (5 μM). The results suggested that the interactions of 9-aminoacridines and Mg^{2+} with the ion channel of the NMDA receptor were not mutually exclusive. Simultaneous occupancy of the NMDA receptor ion channel by Mg^{2+} and a channel-blocking organic cation could be a common mechanism of channel blockade for this receptor under physiological conditions.

The NMDA receptor is thought to play a key role in complex physiological processes such as learning and memory (1) and synaptic plasticity (2), as well as in various pathophysiological processes (3). The control of NMDA receptor activity *in vivo* is complex, as indicated by the number of regulatory factors that act on the receptor. For instance, there is a requirement for a coagonist such as glycine (4), a voltage-dependent blockade of its ion channel by Mg^{2+} (5, 6), a non-voltage-dependent antagonism by Zn^{2+} (7, 8), and a potentiation of channel activation and a low affinity channel blockade by polyamines such as spermine and spermidine (9–11). Previous studies have provided evidence for a single Mg^{2+} binding site located deep within the receptor ion channel (12–14). This has led to the use of Mg^{2+} as a tool to test whether other noncompetitive NMDA receptor antagonists act by binding within the receptor ion channel. Competitive interaction of Mg^{2+} with a test agent is considered evidence that the binding site for the test agent must be located within the channel. Although electrophysiological studies have shown that Mg^{2+} can be used to "protect" the NMDA receptor from blockade by agents such as phencyclidine (15) and MK-801 (16), which are believed to act by binding within the channel, the exact mechanism by which Mg^{2+} protects the channel against blockade by these agents is still unclear. Two possible mechanisms exist that could explain the effects of a channel-blocking agent on the NMDA receptor in the presence of Mg^{2+}. One possibility considers that the interaction of Mg^{2+} with the ion channel could be mutually exclusive, so that the binding of Mg^{2+} within the channel precludes the binding of another cation (such as PCP or MK-801) and only when Mg^{2+} is not occupying the channel can the other cation bind. The second possibility considers that the binding of Mg^{2+} within the channel does not prevent the binding of another cation but simply lowers the affinity of the channel for this cation through electrostatic repulsion or by induction of a conformational change. Obviously, the location of the binding site for Mg^{2+} with respect to that for the test agent is a key determinant. For example, channel-blocking agents that bind deep within the channel would be physically displaced from the

This work was supported in part by a grant from the National Institutes of Health (ES05730).

ABBREVIATIONS: NMDA, *N*-methyl-D-aspartate; THA, 1,2,3,4-tetrahydro-9-aminoacridine; 1,2-PAA, 1,2-propane-bis-9,9′-aminoacridine; 1,4-BAA, 1,4-butane-bis-9,9′-aminoacridine; PCP, 1-(1-phenylcyclhexyl)piperidine; MK-801, (+)-5-methyl-10,11-dihydro-5*H*-dibenzo[*a*,*d*]cyclohepten-5,10-imine maleate; EGTA, ethylene glycol bis(β-aminoethyl ether)-*N*,*N*,*N*′,*N*′-tetraacetic acid; HEPES, 4-(2-hydroxyethyl)-1-piperazineethanesulfonic acid.

channel by Mg^{2+}, whereas peripheral (shallow) channel-blocking agents may not.

In this study, we have been able to demonstrate that 1,2-PAA and 1,4-BAA (Fig. 1) block the open channel of the NMDA receptor with concentration and voltage dependence, as has been previously reported for 9-aminoacridine and THA (17, 18, 19). Furthermore, we provide evidence that Mg^{2+} and the 9-aminoacridines bind to separate sites within the ion channel of the NMDA receptor and that the presence of Mg^{2+} within the channel does not prevent the binding of the 9-aminoacridines. Simultaneous occupation of the NMDA receptor ion channel could be a common mechanism describing the interactions of blocking agents such as MK-801 and PCP in the presence of Mg^{2+}, but this has not been adequately addressed to date. Part of this work has appeared in abstract form (20, 21).

Materials and Methods

Hippocampal cultures. The culture procedures were essentially the same as those reported by Alkondon and Albuquerque (22). Neurons cultured for 7–21 days were used for the experiments.

Single-channel current recordings and analyses. Outside-out patches were obtained by standard patch-clamp techniques (23), using 7–10-MΩ borosilicate microelectrodes with filaments (World Precision Instruments, New Haven, CT) that were coated with Sylgard (Dow Corning Corp., Midland, MI) to reduce noise. Single-channel currents were activated by NMDA (10 μM; Sigma) and glycine (1 μM; Sigma) and monitored using an LM-EPC-7 amplifier (List Electronics, Darmstadt, Germany). The bis-9-aminoacridines (synthesized by Dr. Chester Himel) (24, 25) and THA (Aldrich, Milwaukee, WI) were dissolved in the bathing solution and were applied to the patch by continuous perfusion via an array of capillary tubes, by insertion of the tip of the patch-bearing electrode into the appropriate tube. The currents were stored for off-line analysis on videocassette tapes after passage through a PCM device (Neuro-Corder DR-384; Neuro-Data Instruments Corp., New York, NY). Records were filtered at 3 kHz on playback (eight-pole Bessel, −3 dB, Frequency Devices 90; Frequency Devices, Inc., Haverville, MA), digitized at 12.5 kHz into an IBM AT computer, and then analyzed by the automated IPROC-2 program (Axon Instruments, Foster City, CA). Open events were considered terminated when the amplitude decreased to <50% of the estimated mean single-channel amplitude. The analysis provided the frequency, amplitude, and dwell times of the single-channel currents. Time constants were obtained from exponential least-squares fits of the dwell time histograms, based on a Levenburg-Marquardt algorithm. Bursts were defined as a sequence of openings separated by closed intervals of <4.5 msec. This criterion time was determined according to the method described by Jahr and Stevens (26), where the misclassification of an interburst closed interval as an intraburst closed interval is offset by the misclassification of an intraburst closed interval as an interburst closed interval. The effective cutoff frequency (f_c) of the analysis was 2.9 kHz. This bandwidth does not prevent very brief transitions (lasting less than approximately 58 μsec) from going undetected, so that channel open times and brief closed/blocked times might be slightly overestimated. Values for the respective time constants represent the mean ± standard error from the indicated number (n) of patches. Log-binned histograms were created by importing the events list output from IPROC into the pStat program of pClamp software (Axon) and were not fitted.

Recording solutions. The bathing solution had the following composition (in mM): NaCl, 165; KCl, 5; $CaCl_2$, 1.8; HEPES, 5; D-glucose, 10; and tetrodotoxin, 0.0003 (pH 7.3, 340 mOsM). The solution inside the electrode had the following composition (in mM): CsCl, 80; CsF, 80; Cs-EGTA, 10; and HEPES, 10 (pH 7.3, 330 mOsM). External and internal solutions were prepared with salts purchased from Sigma Chemical Co. (St. Louis, MO). Mg^{2+} concentrations were verified by atomic absorption spectroscopy for both nominally Mg^{2+}-free solutions and solutions where $MgCl_2$ (Mallinkrodt Specialty Chemicals Co., Paris, KY) was added from 10 mM stock solutions.

Single-channel current simulations. Single-channel currents were simulated to evaluate the predictions of various models. The simulations were performed using a computer program (written in C) that was based on a Markov model for channel kinetic behavior. The rate constants used in the simulations were obtained from the data presented here as well as those reported by Jahr and Stevens (26). The models used to test the predictions of the test for competition between Mg^{2+} and 1,2-PAA were extensions of the four-state model reported by Jahr and Stevens (26). For the simultaneous occupancy model, all of the transition rates were fixed except those corresponding to transitions from the Mg^{2+}-blocked state that did not terminate in the open state. The simulated data were then analyzed in the same way as the actual data.

Results

Open-channel blockade by 9-aminoacridines. In outside-out patches from cultured fetal rat hippocampal neurons, NMDA-activated channels predominantly had a conductance of 49.6 ± 0.3 pS. The reversal potential of these single-channel currents was approximately 1.2 mV in solutions containing <0.5 μM Mg^{2+} (Fig. 2). Any additional conductances that may have been present (see Ref. 27) were excluded from the present analysis. In the presence of 1,2-PAA (10 μM), 1,4-BAA (10 μM), or THA (50 μM), the channel lifetimes (τ_{open}) were dramatically shortened at negative holding potentials, whereas very little shortening of the τ_{open} occurred at positive holding potentials (Fig. 3). The control open time histograms at −80 mV were usually best fitted by a single-exponential function, but some histograms were better fitted with a double-exponential function. When double-exponential distributions were observed, the

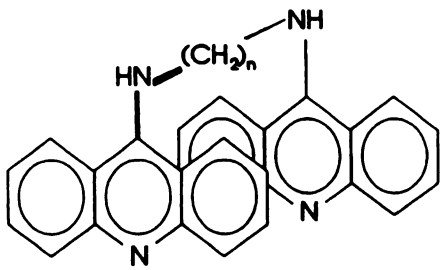

Alkylene bis-9,9′-aminoacridines

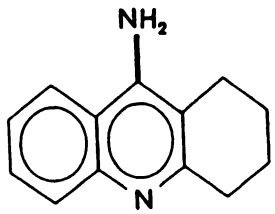

1,2,3,4-tetrahydro-9-aminoacridine

Fig. 1. Structures of the alkylene bis-9,9′-aminoacridines (acridine araphanes) (23) and THA. For the bisacridines n represents the number of CH_2 groups in the alkylene bridge.

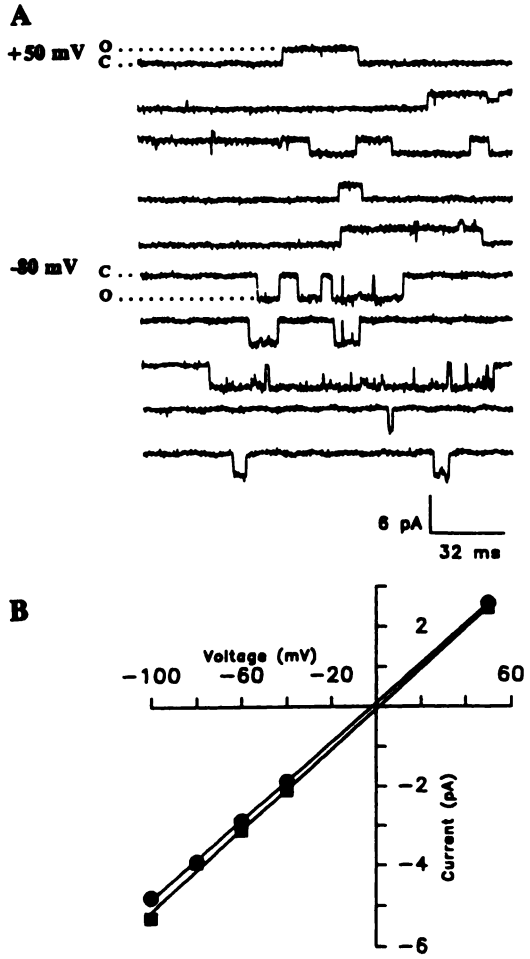

Fig. 2. Characteristics of NMDA-activated single-channel currents in outside-out patches from cultured fetal rat hippocampal neurons. A, *Top*, sample recordings of outward single-channel currents activated by a mixture of NMDA (10 μM) and glycine (1 μM) (holding potential = +50 mV; τ_{open} = 5.12 ± 1.70 msec, n = 4). *Bottom*, sample recordings of inward single-channel currents activated by a mixture of NMDA (10 μM) and glycine (1 μM) (holding potential = −80 mV, τ_{open} = 5.39 ± 0.64 msec, n = 5). *O* and *C*, channel conducting and nonconducting current levels, respectively. The records are discontinuous. B, Current-voltage relationship for NMDA-activated single-channel currents. ●, Currents recorded in solutions containing approximately 5.4 μM Mg^{2+}; ■, currents recorded in nominally Mg^{2+}-free solutions containing <0.5 μM Mg^{2+}. Under either condition the channel conductance was approximately 50 pS; the reversal potentials were −2.0 ± 0.03 mV in solutions containing approximately 5.4 μM Mg^{2+} and 1.2 ± 0.08 mV in nominally Mg^{2+}-free solutions. Each *point* represents the mean ± standard error from three to seven patches, where the error bars were smaller than the symbol size.

time constant of the longer component matched the time constant obtained from fits of other histograms that were clearly single-exponential distributions. In the presence of the 9-aminoacridines, the open time distributions clearly contained only a single component (Fig. 4A). In addition to being voltage dependent, the reductions in τ_{open} were also directly dependent on the 9-aminoacridine concentrations. The concentration and voltage dependencies were consistent with a mechanism of open-channel blockade (28). Applying a sequential model to the blockade of NMDA-activated currents by the 9-aminoacridines, plots of $1/\tau_{open}$ versus the concentration of the acridines (Fig. 5) allowed for the determination of the forward blocking rate constants shown in Table 1. For the bis-9-aminoacridines, the blocking rates approached the limits of diffusion, consistent with a shallow binding site within the channel, whereas the rate for THA blockade was slower and more voltage dependent, suggesting a channel binding site located deeper in the channel.

Because the 9-aminoacridines block the channel in the open state, they should produce a new component in the closed time distributions that would correspond to the channel open but blocked state. All of the 9-aminoacridines altered the closed time distributions (Fig. 6). Note that, although log-binned histograms are shown to illustrate the change in the closed time distributions in the presence of the 9-aminoacridines, fits of linear-binned histograms were used to obtain the closed time constants (see Table 2). Furthermore, the time constants for the blocked state of the channel appeared to be concentration independent (data not shown). THA dramatically increased the number of "closed" events in the distribution of the shortest time constant, revealing that the predominant blocked state was relatively short, with a time constant of approximately 0.16 msec (n = 6) at a holding potential of −80 mV, and indicating that the lower limit (due to the bandwidth of the analysis) of the unblocking rate was approximately 6.2×10^3 sec^{-1} (Fig. 6C; Table 2). In the presence of the bis-9-aminoacridines, the closed time distributions were best fitted by three exponential components, with the longest component most likely representing a combination of the presumed blocked state and the normal channel-closed state. Therefore, the channel-blocked state for the bis-9-aminoacridines was relatively long lived, indicating an unblocking rate on the order of 7 sec^{-1} at −80 mV (Fig. 6, A and B).

The sequential model for open-channel blockade predicts that the channel burst duration (τ_{burst}) increases in the presence of a blocker because channel openings during each receptor activation are interrupted by the channel entering the blocked state, whereas the total time the channel is open and unblocked during each receptor activation should not change (see Ref. 28). Under control recording conditions, the burst-time distributions were fitted best by a double-exponential function, with the longer bursts containing three or four open events on average. In contrast, in the presence of the 9-aminoacridines, the burst-time distributions were clearly a single-exponential function, with the average burst consisting of only one or two open events (Fig. 4B). The reduction in τ_{burst} induced by the bis-9-aminoacridines indicated that the channel-blocked state produced by the bis-9-aminoacridines was much longer than the burst criterion time (4.5 msec), because τ_{burst} became dramatically shorter with increasing concentrations of the bis-9-aminoacridines. Because the bis-9-aminoacridines produce a channel-blocked state that lasts hundreds of milliseconds, the proper burst criterion time should have been close to 1 sec to detect a 'true' burst that included channel blockages by these agents. However, under our recording conditions the result would have been erroneous due to the level of channel activity. THA also reduced τ_{burst}, suggesting either the existence of a long-lived blocked state, in addition to the brief one described above, or the occurrence of a direct transition from the channel-blocked state to a closed state.

Open-channel blockade by Mg^{2+}. Although not the major focus of this study, characterizing the blockade by Mg^{2+} of NMDA-activated currents in our system was necessary to study the effects of Mg^{2+} on channel blockade by the 9-aminoacridines, especially in light of the recent evidence for varying

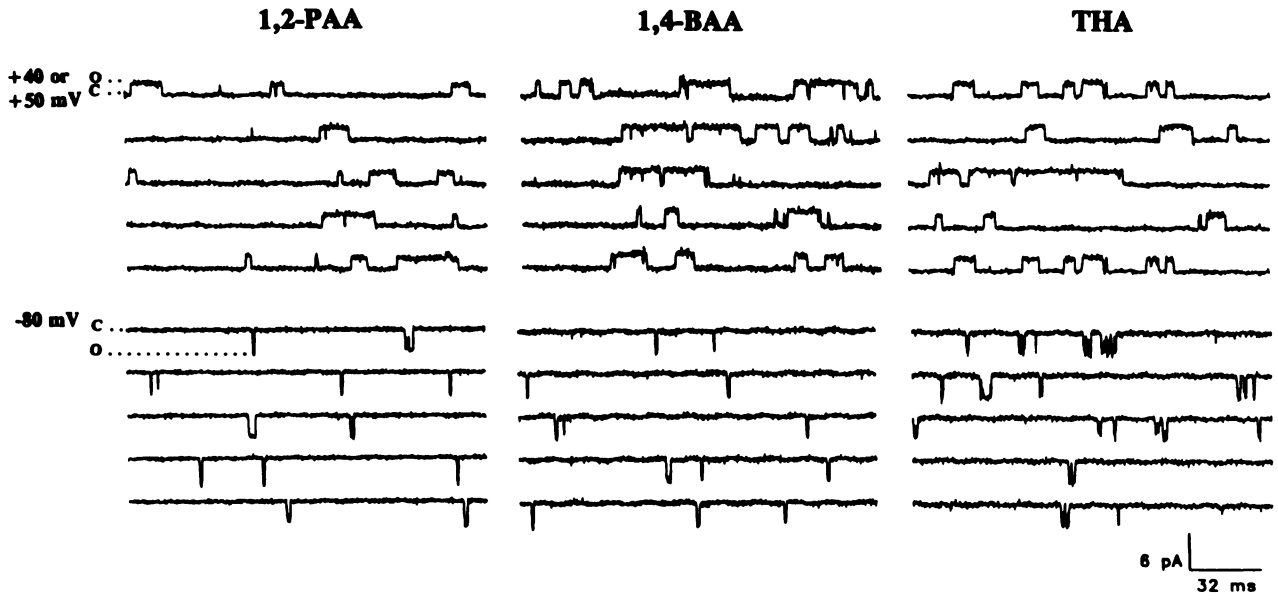

Fig. 3. Voltage-dependent reduction in NMDA-activated channel open times in the presence of 9-aminoacridines. Sample recordings of currents activated by a mixture of NMDA (10 μM) and glycine (1 μM) in the presence of 1,2-PAA (10 μM) (*left*) (*bottom*, holding potential = −80 mV, τ_{open} = 0.76 ± 0.05 msec, n = 3; *top*, holding potential = +40 mV, τ_{open} = 3.82 ± 0.92 msec, n = 3), 1,4-BAA (10 μM) (*middle*) (*bottom*, holding potential = −80 mV, τ_{open} = 0.66 ± 0.04 msec, n = 4; *top*, holding potential = +50 mV, τ_{open} = 3.62 ± 0.18 msec, n = 4), or THA (50 μM) (*right*) (*bottom*, holding potential = −80 mV, τ_{open}= 0.48 ± 0.01 msec, n = 4; *top*, holding potential = +50 mV, τ_{open}= 4.98 ± 0.98 msec, n = 3) are shown. *O* and *C*, channel conducting and nonconducting current levels, respectively. The records are discontinuous.

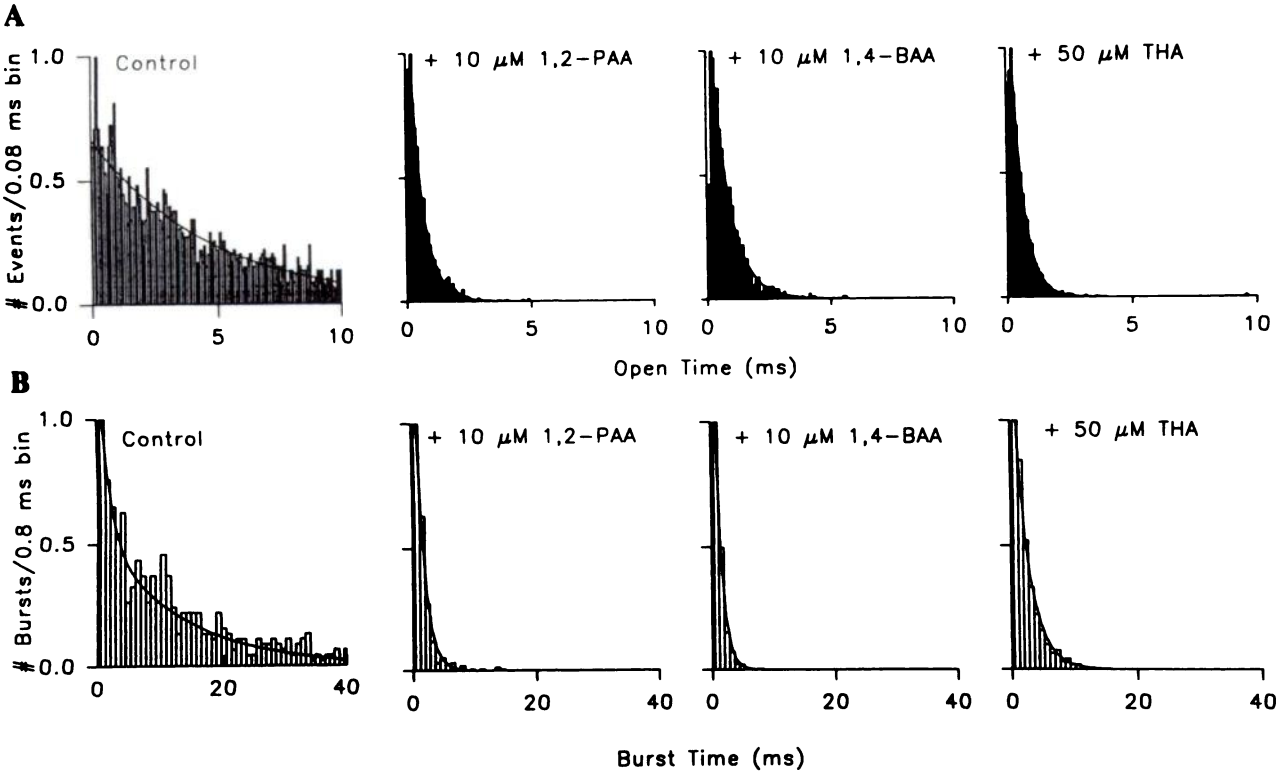

Fig. 4. Representative histograms of open and burst times at a holding potential of −80 mV, in the presence and absence of the 9-aminoacridines. A, Open-time histograms for NMDA-activated channel activity under the indicated conditions. The values of τ_{open} are given in the legends to Fig. 1 (control) and Fig. 3 (in presence of 9-aminoacidine). B, Burst-time histograms for NMDA-activated channel activity under the indicated conditions. Control, τ_{burst} = 1.67 ± 0.60 and 17.93 ± 1.80 msec, n = 5; 1,2-PAA (10 μM), τ_{burst} = 1.29 ± 0.09 msec, n = 3; 1,4-BAA (10 μM), τ_{burst} = 0.78 ± 0.03 msec, n = 4; THA (50 μM), τ_{burst} = 2.05 ± 0.12 msec, n = 4. All of the histograms were normalized to the bin containing the greatest number of events. *Solid lines*, exponential fits to the histograms.

sensitivities of different recombinant NMDA receptors to blockade by Mg^{2+} (29–31). Mg^{2+} was found to cause a voltage- and concentration-dependent reduction in τ_{open} (Fig. 7, A and B, a). This finding was consistent with a mechanism of open-channel blockade, as has been previously reported for the effects of Mg^{2+} on NMDA-activated currents (5, 6, 26). The

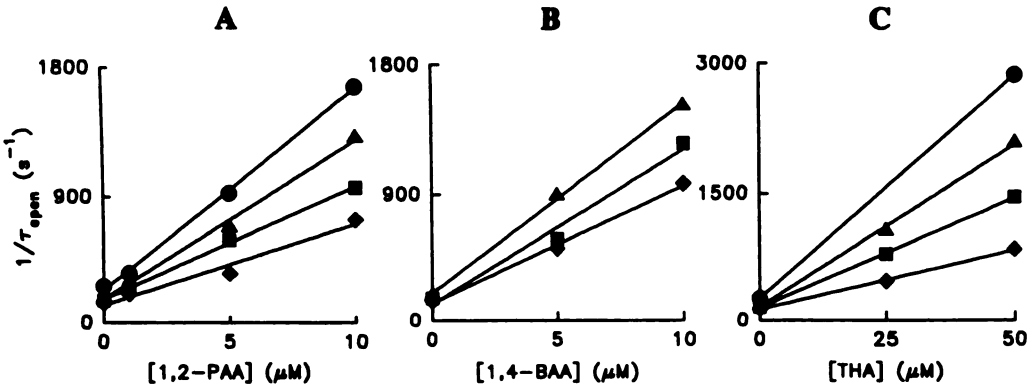

Fig. 5. Concentration and voltage dependence of channel open time in the presence of the 9-aminoacridines. The effects on channel open time of various concentrations of the 9-aminoacridines were determined at various holding potentials, i.e., −40 (♦), −60 (■), −80 (▲), and −100 mV (●). A, $1/\tau_{open}$ versus [1,2-PAA]; B, $1/\tau_{open}$ versus [1,4-BAA]; C, $1/\tau_{open}$ versus [THA]. Each *point* represents the mean from three to seven patches. The *solid lines* correspond to least-squares fits of the data to the equation $1/\tau_{open} = \alpha + k_+[9\text{-aminoacridine}]$, where α is the channel closing rate (ordinate intercept) and k_+ represents the forward blocking rate constant at that holding potential. The slope of each line corresponds to the forward blocking rate constant at that holding potential. At −80 mV, the rate constants were 1.1×10^8, 1.3×10^8, and 3.8×10^7 M^{-1} sec^{-1} for 1,2-PAA, 1,4-BAA, and THA, respectively.

TABLE 1

Blocking rate constants determined according to a model of open-channel blockade

Channel blocker	Forward rate constant, k_+
	M^{-1} sec^{-1}
1,2-PAA	3.3×10^7 exp(−*V*/67)[a]
1,4-BAA	5.3×10^7 exp(−*V*/83)
THA	7.7×10^6 exp(−*V*/53)
Mg^{2+}	1.4×10^6 exp(−*V*/21)

[a] *V*, holding potential (in mV).

concentration dependence of the reduction in τ_{open} was linear over the range of Mg^{2+} concentrations studied and allowed for determination of the forward blocking rate constant (Fig. 7, B, a; Table 1). The Mg^{2+}-blocked state was found to be voltage dependent but concentration independent (Fig. 7, B, b) and had a time constant of 1.03 ± 0.06 msec (n = 4) at −80 mV. From the relationship $K_d = k_-/k_+$, where k_- and k_+ represent the unblocking and blocking rate constants, respectively, the K_d values for Mg^{2+} at various holding potentials were determined (Fig. 7, B, c). The τ_{burst} measured in the presence of added Mg^{2+} was shorter than that found under nominally Mg^{2+}-free conditions ([Mg^{2+}] < 0.5 μM), and the reductions in τ_{burst} were somewhat concentration dependent (Fig. 7, B, d).

Test for competition between Mg^{2+} and 9-aminoacridines in channel blockade of the NMDA receptor. The experiments that characterized the effects of 9-aminoacridines described above were performed in nominally Mg^{2+}-free solutions containing <0.5 μM Mg^{2+}. Additional experiments with 9-aminoacridines were performed in solutions containing Mg^{2+} (~5 μM), and the results were qualitatively the same as those presented above, in that the 9-aminoacridines caused a concentration- and voltage-dependent reduction in τ_{open}. However, the concentration dependence was not linear (Fig. 8). This finding raised the question of whether Mg^{2+} and the 9-aminoacridines were competing for a single site within the open channel of the receptor or whether the binding of Mg^{2+} and a 9-aminoacridine could occur simultaneously. To differentiate between these two possibilities, experiments were designed to test for competition (see Ref. 32) between Mg^{2+} and 1,2-PAA for binding within the channel. NMDA-activated single-channel currents were recorded in the presence of 1,2-PAA (5 μM) and varying concentrations of Mg^{2+} (~0–50 μM). For these experiments, the τ_{burst} were analyzed using a criterion time (4.5 msec) that was based on the Mg^{2+}-blocked state. For such an analysis, the bursts contained only channel blockages caused by Mg^{2+} (fast) and excluded channel blockages caused by 1,2-PAA (slow). The τ_{burst} in the presence of both Mg^{2+} and 1,2-PAA was compared with the τ_{burst} in the presence of only 1,2-PAA (Fig. 9). As shown in Fig. 9, the burst distribution in the presence of 1,2-PAA was a single-exponential function but as the concentration of Mg^{2+} was increased the distribution became a double-exponential function. At 25 and 50 μM Mg^{2+}, the faster component had a time constant almost identical to τ_{open}. This meant that the faster component simply represented isolated, single-event bursts. Doubling the burst criterion time slightly altered the τ_{burst} but did not remove the faster component. Therefore, the longer τ_{burst} was thought to represent the bursts that included channel blockages due to Mg^{2+} and excluded those due to 1,2-PAA. The ratios of these τ_{burst} values, when plotted against the concentration of Mg^{2+}, increased slightly as the concentration of Mg^{2+} was increased (Fig. 10). However, a much larger increase in the τ_{burst} would be expected for a mutually exclusive competition between Mg^{2+} and 1,2-PAA for binding within the channel (Fig. 10; see Discussion). If the binding of 1,2-PAA (a "slow" unblocker) and Mg^{2+} (a "fast" unblocker) within the channel were mutually exclusive, then the ratio of τ_{burst} in the presence of both Mg^{2+} and 1,2-PAA to τ_{burst} in the presence of only 1,2-PAA should have increased linearly as the concentration of Mg^{2+} increased, because the burst criterion was based on the Mg^{2+}-blocked state.

Discussion

The present results demonstrate that the bis-9-aminoacridines 1,2-PAA and 1,4-BAA, as well as THA, are open-channel blockers of the NMDA receptor. This is evident from the voltage- and concentration-dependent reduction of τ_{open} induced by the acridines. Both 1,2-PAA and 1,4-BAA are more effective in reducing τ_{open} than is THA, which is reflected in the forward blocking rate constants (see Table 1). Additionally, the channel-blocked state produced by the bis-9-aminoacridines is relatively stable, with a duration of approximately 150–

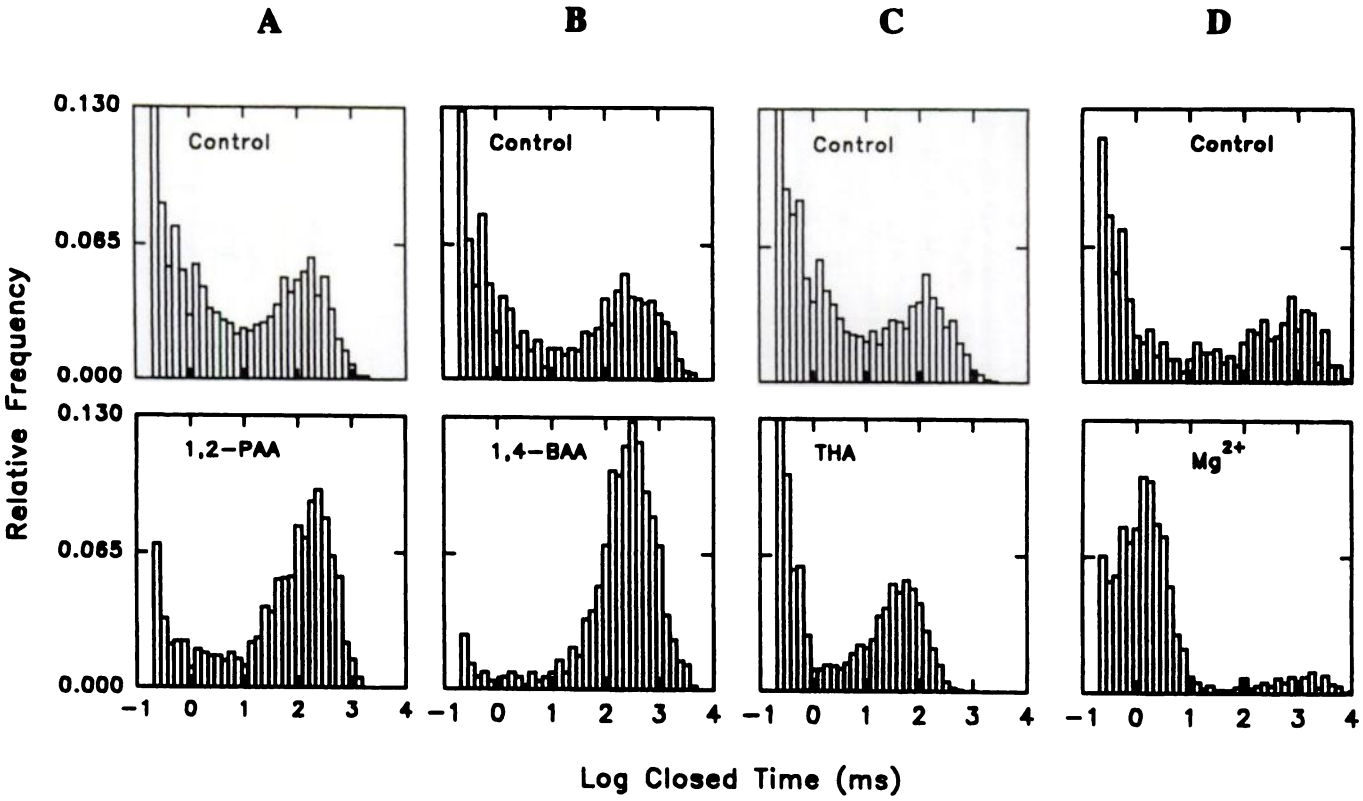

Fig. 6. Representative log-binned closed-time histograms in the absence and presence of 9-aminoacridines. A, Control (*top*) and in the presence of 5 μM 1,2-PAA (*bottom*); B, control (*top*) and in the presence of 10 μM 1,4-BAA (*bottom*); C, control (*top*) and in the presence of 50 μM THA (*bottom*); D, control (*top*) and in the presence of 50 μM Mg^{2+} (*bottom*). All of the histograms contained 8 bins/decade. The relative frequency was the number of events normalized to the number of open events in that recording. For the THA histograms, this had the effect of de-emphasizing the peak in the distribution due to the THA-blocked state. When the number of events was instead normalized to the length of the recording, the peak corresponding to the THA-blocked state was clear, while those of the bis-9-aminoacidine were deemphasized. This was because the frequencies of channel openings in the presence of the bis-9-aminoacridines ("slow" unblockers) were reduced by approximately 50%, whereas THA (a "fast" unblocker) increased the frequency of openings by approximately 300% and Mg^{2+} (a "fast" unblocker) increased the frequency of openings by approximately 200%. A-D were obtained from different patches held at −80 mV in nominally Mg^{2+}-free solutions except where Mg^{2+} was added.

TABLE 2

Channel closed time constants in the presence and absence of 9-aminoacridines

Values represent the means ± standard errors for five to nine patches.

Channel blocker	Channel closed time constants[a]			
	τ_1	τ_2	τ_3	τ_4
	msec			
Control	0.19 ± 0.03	1.26 ± 0.10	24.5 ± 3.4	294 ± 56
THA	0.16 ± 0.01	2.10 ± 0.29	52.3 ± 9.0	161 ± 32
1,2-PAA	0.08 ± 0.01	0.99 ± 0.22	—[b]	187 ± 26
1,4-BAA	0.24 ± 0.07	2.40 ± 0.29	—	228 ± 31

[a] Holding potential, −80 mV.
[b] Component not present.

200 msec at −80 mV, and therefore results in a shortening of τ_{burst} as we have defined it. THA, in contrast to the bis-9-aminoacridines, produces a blocked state having a duration of approximately 0.16 msec at −80 mV (see Table 2). Because the duration of the THA-blocked state is much briefer than the burst criterion time, THA should have caused an increase in τ_{burst}. However, THA, similarly to the bis-9-aminoacridines, reduces τ_{burst}. Two possible mechanisms could account for the shortening of τ_{burst} by THA, i.e., 1) the channel could undergo a direct transition from the blocked state into a closed state or 2) THA could produce a long-duration blocked state, in addition to the brief blocked state, which would effectively end a burst when entered. We favor the latter explanation, because this mechanism is consistent with the "delayed current peaks" observed in NMDA-activated whole-cell currents when THA and NMDA are rapidly removed (see Ref. 17). Also, one of the longer closed-time constants (see Table 2) in the presence of THA could have been due to an additional, more stable, blocked state, but this could not be clearly resolved.

Although only a relatively narrow concentration range of Mg^{2+} has been studied, the effects of Mg^{2+} on NMDA-activated single-channel currents are similar to those reported previously (5, 6, 13, 26). Consistent with a mechanism of open-channel blockade, Mg^{2+} causes a concentration- and voltage-dependent reduction in τ_{open}. The forward rate constant for blockade by Mg^{2+} based on this model is $1.4 \times 10^6 \exp(-V/21)$ M^{-1} sec^{-1}. The time constant of the Mg^{2+}-blocked state corresponds to an unblocking rate constant of $3.6 \times 10^3 \exp(V/62)$ sec^{-1}. Although most of the effects of Mg^{2+} are consistent with a mechanism of open-channel blockade, Mg^{2+} did not cause an increase in τ_{burst}, an obvious departure from the predictions of a sequential model for open-channel blockade. Two mechanisms have been postulated that could explain this deviation, i.e., 1) a transition from the Mg^{2+}-blocked state into a channel-closed state takes place before Mg^{2+} dissociates (26) or 2) a transition into a long-lived Mg^{2+}-blocked state occurs in addition to the known short-duration blocked state transitions (13). Either of these transitions occurring at an appropriate rate could explain why Mg^{2+} does not increase τ_{burst}. However, the second possibility seems

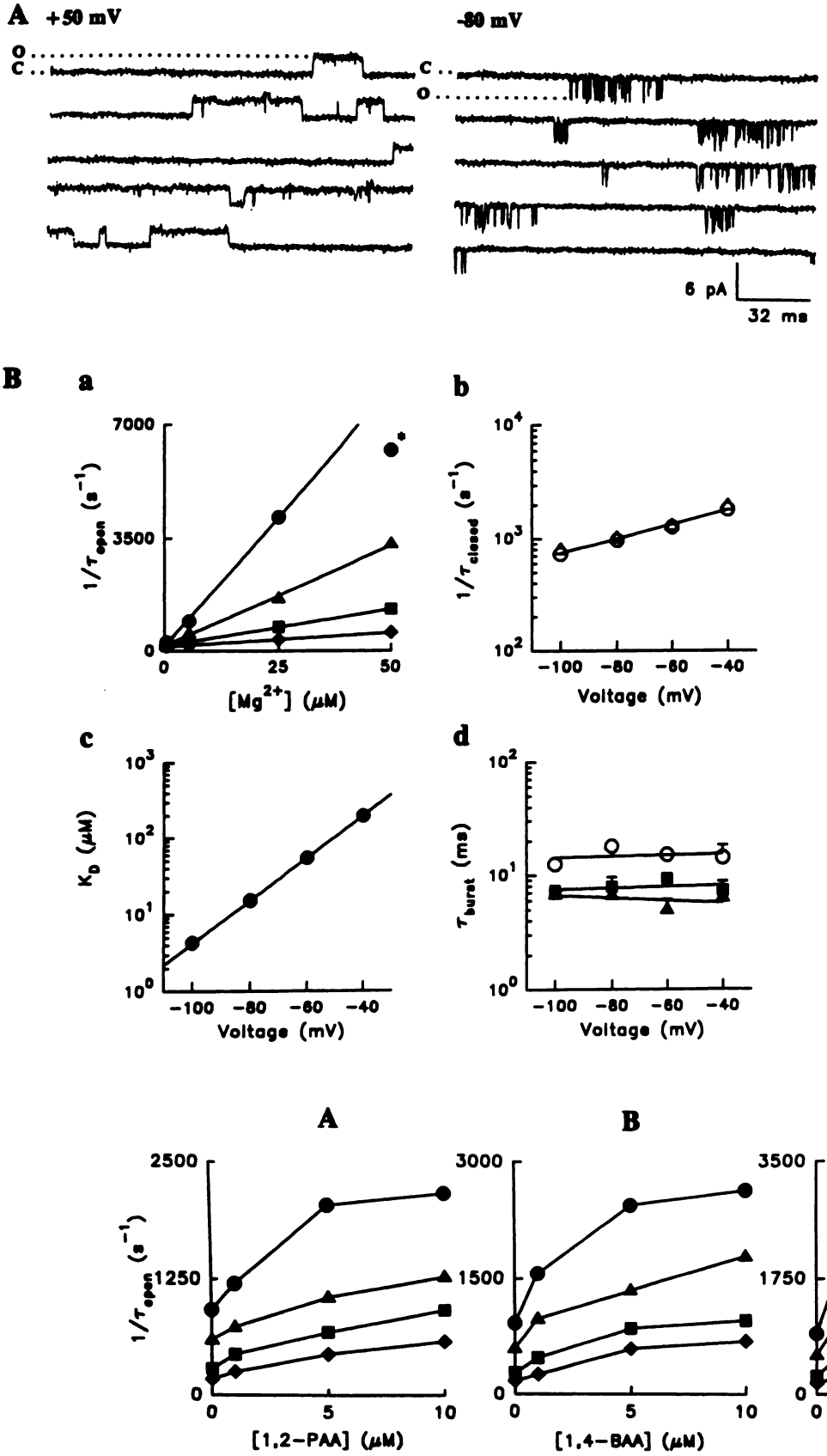

Fig. 7. Mg^{2+} blockade of NMDA-activated single-channel currents. A, Sample recordings of single-channel currents activated by a mixture of NMDA (10 μM) and glycine (1 μM), in the presence of Mg^{2+} (50 μM), at holding potentials of −80 and +50 mV. B, a, Mg^{2+} blocking rate. Plot of $1/\tau_{open}$ versus concentration of Mg^{2+} at holding potentials of −40 (♦), −60 (■), −80 (▲), and −100 mV (●). *Solid lines*, least-squares fits of the data to the equation $1/\tau_{open} = \alpha + k_+[Mg^{2+}]$, where α is the channel closing rate (ordinate intercept) and k_+ represents the forward blocking rate constant at that holding potential. *, Point that was not included in the fit because it not only was inconsistent with the blocking rates at lower concentrations but also resulted in an affinity constant that was inconsistent with those shown in c. Each *point* represents data from three to five patches. b, Mg^{2+} unblocking rate. Plot of $1/\tau_{closed}$ versus holding potential at 25 μM Mg^{2+} (○) and 50 μM Mg^{2+} (△). Each *point* represents the data from three to five patches. c, Voltage dependence of the affinity constant of the NMDA receptor for Mg^{2+}. K_d values were determined from the relationship $K_d = k_-/k_+$, where k_- and k_+ are the unblocking and blocking rates of Mg^{2+}, respectively, estimated from the single-channel kinetics in the presence of various concentrations of Mg^{2+} (up to 50 μM) and assuming a mechanism of open-channel blockade. *Solid line*, least-squares fit to the data corresponding to the equation $K_d = 2.6 \times 10^{-3} \exp(V/16)$ M^{-1} sec^{-1}, where V is the holding potential (in mV). The *points* were calculated from the data shown in a and b. d, Voltage dependence of the channel burst times under nominally Mg^{2+}-free conditions (○) and in the presence of 25 μM Mg^{2+} (■) and 50 μM Mg^{2+} (▲). Each *point* represents the mean ± standard error from three to five patches.

Fig. 8. Effect of Mg^{2+} on concentration-dependent reduction of the channel open time induced by the 9-aminoacridines. The concentration of Mg^{2+} in these solutions was approximately 5.4 μM. The effects of the 9-aminoacridines on channel open time were determined at various holding potentials, i.e., −40 (♦), −60 (■), −80 (▲), and −100 mV (●). A, $1/\tau_{open}$ versus [1,2-PAA]; B, $1/\tau_{open}$ versus [1,4-BAA]; C, $1/\tau_{open}$ versus [THA]. The *lines* for each plot were drawn simply to connect the data points. Each *point* represents the mean from three to seven patches.

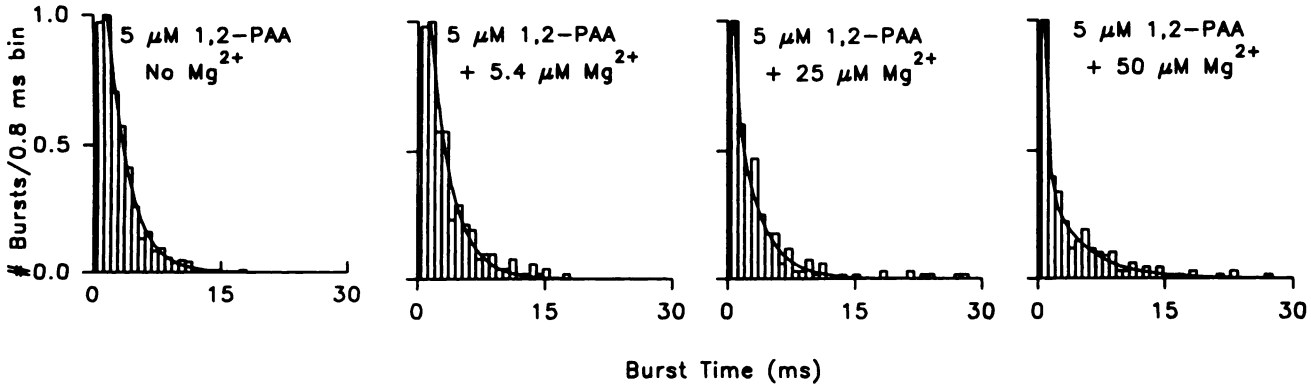

Fig. 9. Representative histograms of the effect of Mg^{2+} on 1,2-PAA-induced reduction in NMDA-activated τ_{burst}. At a fixed concentration of 1,2-PAA (5 μM), as the concentration of Mg^{2+} was progressively increased the distribution of channel burst time became a double-exponential function, with the slower component increasing only slightly. In the presence of no added Mg^{2+}, τ_{burst} was 2.18 ± 0.04 msec (n = 3); in the presence of 5.4 μM Mg^{2+}, τ_{burst} was 2.85 ± 0.10 msec (n = 5); in the presence of 25 μM Mg^{2+}, τ_{burst} values were 0.49 ± 0.13 msec (fast component) and 3.29 ± 0.08 msec (slow component) (n = 3); in the presence of 50 μM Mg^{2+}, τ_{burst} values were 0.41 ± 0.10 msec (fast component) and 3.92 ± 0.16 msec (slow component) (n = 3). *Solid lines*, exponential fits to the histograms. All of the histograms were normalized to the bin containing the greatest number of bursts.

unlikely, because the closed-time distributions at all Mg^{2+} concentrations indicate only a single blocked state (i.e., there is no evidence for a time constant that would correspond to a second, longer, blocked state). This leads us to favor a mechanism of blockade involving a single open-channel-blocked state that allows for a direct transition into a channel-closed state.

Several biochemical and electrophysiological studies have reported that Mg^{2+} can alter the interactions of organic cations such as MK-801 (16, 33) and PCP (15) with the NMDA receptor in a competitive way. Those studies demonstrated that the affinity for the organic cation is apparently reduced in the presence of Mg^{2+}. However, the apparent reduction in affinity for the organic cation could represent at least two possible mechanisms. First, the reduced affinity could be due to a mutually exclusive competition for the channel (model I),

$$\begin{array}{c} R^* + D \rightleftarrows R^*D \\ +Mg^{2+} \Updownarrow \\ R^*Mg^{2+} \end{array} \qquad \text{(model I)}$$

where R* represents the open state of the receptor and D represents an organic cation. Note that for simplicity the closed states leading to the open state are not shown. Alternatively, the reduced affinity could be due to simultaneous binding of both Mg^{2+} and the organic cation (model II),

$$\begin{array}{c} R^* + D \rightleftarrows R^*D \\ +Mg^{2+} \Updownarrow \\ R^*Mg^{2+} + D \rightleftarrows R^*Mg^{2+}D \end{array} \qquad \text{(model II)}$$

where the presence of Mg^{2+} within the channel reduces the affinity for the organic cation, possibly via electrostatic repulsion or a conformational change within the channel. The symbols for model II are the same as for model I. Few studies have directly addressed the question of whether Mg^{2+} and channel-blocking organic cations can simultaneously occupy the channel of the NMDA receptor. One such biochemical study reports that, under conditions of low ionic strength, Mg^{2+} apparently increases the rate of MK-801 association to and dissociation from the channel (33). In that study, the effects of Mg^{2+} on MK-801 binding within the channel were attributed to a non-competitive interaction at different sites for each cation that allowed for an allosteric modulation of MK-801 binding by Mg^{2+}. Because the effects of the 9-aminoacridines on NMDA-activated single-channel currents indicate a blockade of the open channel, we attempted to address the issue of whether Mg^{2+} acts in a competitive manner with 9-aminoacridines for binding within the channel of the receptor, using the single-channel patch-clamp technique. Our approach is modeled after that reported by Miller (32). Because the bis-9-aminoacridines have dissociation rates 2 orders of magnitude slower than that of Mg^{2+}, determination of whether the binding of Mg^{2+} and 1,2-PAA is mutually exclusive is made possible by defining the burst using a criterion time based on the Mg^{2+}-blocked state and then analyzing τ_{burst} at a fixed concentration of 1,2-PAA while increasing the Mg^{2+} concentration. If the interactions of Mg^{2+} and 1,2-PAA with the channel are mutually exclusive,

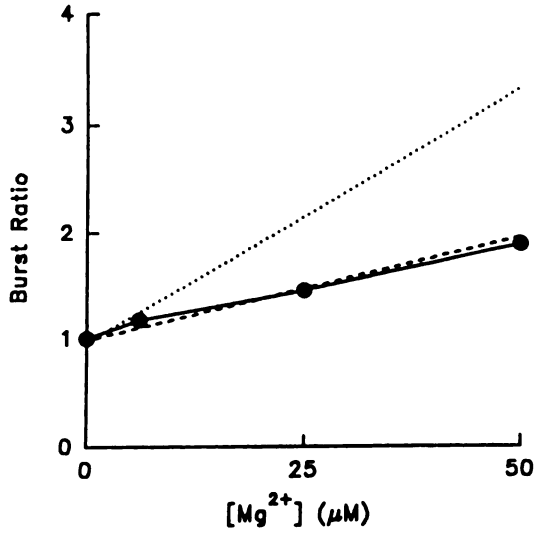

Fig. 10. Test for competition between Mg^{2+} and 1,2-PAA. Plots of the ratio of τ_{burst} in the presence of Mg^{2+} and 1,2-PAA (5 μM) to τ_{burst} in the presence of only 5 μM 1,2-PAA (i.e., burst ratio, τ_{burst} for 1,2-PAA plus Mg^{2+}/τ_{burst} for 1,2-PAA versus [Mg^{2+}]) are shown. The criterion time for the burst analysis was 4.5 msec and >1 order of magnitude shorter than the blocked state by 1,2-PAA. ———, Relationship for the actual data points, drawn simply between each point; · · · · ·, predicted ratios for a model based on competition for the same channel site between 1,2-PAA and Mg^{2+}; – – –, relationship for a model allowing for simultaneous occupancy by 1,2-PAA and Mg^{2+}. The *points* predicted by the models were obtained by simulating channel activity, as described in Materials and Methods.

then defining a burst in such a way makes τ_{burst} reflect the probability that the channel is not occupied by 1,2-PAA and τ_{burst} should depend linearly on the Mg^{2+} concentration. The predictions of a mutually exclusive model and a simultaneous occupancy model for describing the effects of coadministration of Mg^{2+} and 1,2-PAA on the channel-burst duration can be seen in Fig. 10. A comparison of the actual experimental results with the predictions of each model suggests that Mg^{2+} and 1,2-PAA interact with distinct sites within the channel of the NMDA receptor and that they may occupy the channel simultaneously.

Two possible problems with this test for competition between Mg^{2+} and 1,2-PAA could be that Mg^{2+} might reduce τ_{burst} by a mechanism unrelated to channel blockade or that the mechanism by which Mg^{2+} reduces τ_{burst} might result in a closed time constant that is indistinguishable from that for the long-lived blocked state induced by the bis-9-aminoacridines. The experiments performed in the presence of Mg^{2+} alone, however, suggest that if these mechanisms exist they are not significant in the concentration range used in this study. Although Mg^{2+} does not increase τ_{burst}, as predicted by the sequential model, τ_{burst} in the presence of 50 μM Mg^{2+} (the highest test concentration) alone is still 4-fold longer than that in the presence of 5 μM 1,2-PAA alone, suggesting that the experiment should still be able to reveal the nature of the interaction between Mg^{2+} and 1,2-PAA. Moreover, as mentioned above, it has been demonstrated that simply allowing the channel to close from its Mg^{2+}-blocked state would be adequate to explain why Mg^{2+} does not increase burst length (26), and this transition does not affect the predictions of the test for competition unless the transition rate between the Mg^{2+}-blocked state and the closed state is >4-fold faster than the value reported.

Additional support for a mechanism of simultaneous occupancy comes from the nonlinearity of the plots of $1/\tau_{open}$ versus 9-aminoacridine concentration in the presence of low Mg^{2+} concentrations. Any model based solely on mutually exclusive interactions with the open channel of the receptor for both Mg^{2+} and 1,2-PAA does not predict such nonlinearity. For such a model, if the concentration of Mg^{2+} is held constant while the concentration of 1,2-PAA is varied, a linear relationship between $1/\tau_{open}$ and the concentration of 1,2-PAA would be expected. However, as can be seen in Fig. 8, this is not the case. Conversely, if the concentration of 1,2-PAA is held constant while the concentration of Mg^{2+} is altered, the relationship between $1/\tau_{open}$ and the concentration of Mg^{2+} should also be linear, but it is not (data not shown). One explanation for this behavior might be that the binding site for 1,2-PAA also serves as a low affinity site for interaction with Mg^{2+}, in addition to the high affinity site located deeper within the channel. However, the nonlinearity in the $1/\tau_{open}$ versus concentration of 9-aminoacridine plots can also be explained by a model involving interaction of the acridines with the Mg^{2+}-blocked state of the receptor. The interaction of the acridines with the Mg^{2+}-blocked state of the receptor could be modeled in three ways, i.e., 1) 1,2-PAA binds to the Mg^{2+}-blocked state (model II) and therefore generates a new blocked state, 2) the acridines simply facilitate the transition between the Mg^{2+}-blocked state and a channel-closed state, or 3) the 9-aminoacridines bind to the Mg^{2+}-blocked state and increase Mg^{2+} permeation through the channel by electrostatic repulsion. It is difficult to clearly distinguish among these possibilities using single-channel analysis, because these mechanisms involve transitions between nonconducting states. Preliminary results of whole-cell patch-clamp experiments indicate that Mg^{2+} alters the unblocking rate of 1,2-PAA, which is consistent with the first possibility of a new blocked state.[1] Additional whole-cell experiments should be helpful in resolving this issue.

Because the binding of Mg^{2+} within the channel of the NMDA receptor does not seem to prevent the binding of the 9-aminoacridines, simultaneous occupation of the channel by both Mg^{2+} and 1,2-PAA is a likely possibility. This at first seems surprising, considering the bulk of the bis-9-aminoacridines (see Ref. 25) and considering the number of charges involved (two for Mg^{2+} and at least two for the bisacridines (24). However, this seems less unlikely if the binding site for the 9-aminoacridines is located far from that for Mg^{2+}. In fact, the data presented here are entirely consistent with this line of reasoning. Using the voltage dependence of the K_d for Mg^{2+} (approximately e-fold for 16 mV), we estimate the distance across the membrane electric field at which Mg^{2+} binding occurs (34) to be approximately 80% of the way, and the binding site therefore lies very deep within the channel. Although the voltage dependence of the binding affinity for the 9-aminoacridines has not been determined due to the uncertainty in estimating the duration of the channel-blocked state, the weak voltage dependence of the forward blocking rate constant is consistent with binding of these agents at a shallow site within the channel. The deep and shallow locations of the binding sites for Mg^{2+} and the 9-aminoacridines, respectively, would reduce the interactions between them and would therefore make simultaneous occupation of the channel possible.

In summary, both Mg^{2+} and the 9-aminoacridines interact with the open channel of the NMDA receptor. The binding of Mg^{2+} seems to be at a site located deep within the channel, whereas the binding of the bis-9-aminoacridines seems to occur at a shallow site. The separation between these two binding sites allows for the simultaneous binding of Mg^{2+} and the 9-aminoacridines within the channel. Simultaneous occupation of the NMDA receptor channel may also occur with other organic cations and might be a more accurate description of channel blockade by organic cations under conditions where physiological concentrations of Mg^{2+} are present.

Acknowledgments

The authors wish to thank Ms. Barbara Marrow, Mr. Ben Cumming, and Ms. Mabel Zelle for expert technical assistance, Dr. Joseph Montes for performing the Mg^{2+} measurements, and Ms. Edna F. R. Pereira for comments on the manuscript.

References

1. Morris, R. G. M., E. Anderson, G. S. Lynch, and M. Bandry. Selective impairment of learning and blockade of long-term potentiation by an *N*-methyl-D-aspartate receptor antagonist, AP5. *Nature (Lond.)* **319**:774–776 (1986).
2. Kleinschmidt, A., M. F. Bean, and W. Singer. Blockade of "NMDA" receptors disrupts experience-dependent plasticity of kitten striate cortex. *Science (Washington D. C.)* **238**:355–358 (1987).
3. Choi, D. W. Glutamate neurotoxicity and diseases of the nervous system. *Neuron* **1**:623–634 (1988).
4. Dingledine, R., N. W. Kleckner, and C. J. McBain. The glycine coagonist site of the NMDA receptor. *Adv. Exp. Med. Biol.* **268**:17–26 (1990).
5. Nowak, L., P. Bregestovski, P. Ascher, A. Herbet, and A. Prochiantz. Magnesium gates glutamate-activated channels in mouse central neurones. *Nature (Lond.)* **307**:462–465 (1984).
6. Mayer, M. L., G. L. Westbrook, and P. B. Guthrie. Voltage-dependent block by Mg^{2+} of NMDA responses in spinal cord neurones. *Nature (Lond.)* **309**:261–263 (1984).

[1] M. E. Nelson and E. X. Albuquerque, unpublished observations.

7. Peters, S., J. Koh, and D. W. Choi. Zinc selectively blocks the action of *N*-methyl-D-aspartic acid on cortical neurons. *Science (Washington D. C.)* **236**:589–593 (1987).
8. Westbrook, G. L., and M. L. Mayer. Micromolar concentrations of Zn^{2+} antagonize NMDA and GABA responses of hippocampal neurons. *Nature (Lond.)* **328**:640–643 (1987).
9. Ranson, R. W., and N. L. Stec. Cooperative modulation of [^{3}H]-MK-801 binding to the *N*-methyl-D-aspartate receptor-ion channel complex by L-glutamate, glycine, and polyamines. *J. Neurochem.* **51**:830–836 (1988).
10. Williams, K., V. L. Dawson, C. Ramano, M. H. Dichter, and P. B. Molinoff. Characterization of polyamines having agonist, antagonist, and inverse agonist effects at the polyamine recognition site of the NMDA receptor. *Neuron* **5**:199–208 (1990).
11. Araneda, R. C., R. S. Zukin, and M. V. L. Bennett. Effects of polyamines on NMDA-induced currents in rat hippocampal neurons: a whole-cell and single-channel study. *Neurosci. Lett.* **152**:107–112 (1993).
12. Mayer, M. L., and G. L. Westbrook. Permeation and block of *N*-methyl-D-aspartic acid receptor channels by divalent cations in mouse cultured central neurones. *J. Physiol. (Lond.)* **394**:501–527 (1987).
13. Ascher, P., and L. Nowak. The role of divalent cations in the *N*-methyl-D-aspartate responses of mouse central neurones in culture. *J. Physiol. (Lond.)* **399**:247–266 (1988).
14. Mori, H., H. Masaki, T. Yamakura, and M. Mishina. Identification by mutagenesis of Mg^{2+}-block site of the NMDA receptor channel. *Nature (Lond.)* **358**:673–675 (1992).
15. Lerma, J., R. S. Zukin, and V. L. Bennett. Interaction of Mg^{2+} and phencyclidine in use-dependent block of NMDA channels. *Neurosci. Lett.* **123**:187–191 (1991).
16. Huettner, J. E., and B. P. Bean. Block of *N*-methyl-D-aspartate-activated current by the anticonvulsant MK-801: selective binding to open channels. *Proc. Natl. Acad. Sci. USA* **85**:1307–1311 (1988).
17. Costa, A. C. S., and E. X. Albuquerque. Dynamics of the actions of tetrahydro-9-aminoacridine and 9-aminoacridine on glutamatergic currents: concentration-jump studies in cultured rat hippocampal neurons. *J. Pharmacol. Exp. Ther.* **268**:503–514 (1994).
18. Hershkowitz, N., and M. Rogawski. Tetrahydroaminoacridine block of *N*-methyl-D-aspartate-activated cation channels in cultured hippocampal neurons. *Mol. Pharmacol.* **39**:592–598 (1991).
19. Benveniste, M., and M. L. Mayer. Channel block by 9-aminoacridine prevents dissociation of NMDA and glycine from NMDA receptors. *Soc. Neurosci. Abstr.* **19**:278 (1993).
20. Nelson, M. E., E. F. R. Pereira, and E. X. Albuquerque. Sensitivity of *N*-methyl-D-aspartate receptors to 9-aminoacridines. *Soc. Neurosci. Abstr.* **18**:1510 (1992).
21. Nelson, M. E., J. G. Montes, and E. X. Albuquerque. Effects of magnesium on open-channel blockade by 9-aminoacridines. *Soc. Neurosci. Abstr.* **19**:1136 (1993).
22. Alkondon, M., and E. X. Albuquerque. Diversity of nicotinic acetylcholine receptors in rat hippocampal neurons. I. Pharmacological evidence for distinct structural subtypes. *J. Pharmacol. Exp. Ther.* **265**:1455–1473 (1993).
23. Hamill, O. P., A. Marty, E. Neher, B. Sakmann, and F. J. Sigworth. Improved patch-clamp techniques for high-resolution current recording from cells and cell-free membrane patches. *Pflügers Arch.* **391**:85–100 (1981).
24. Himel, C. M., J. L. Taylor, C. Pape, D. B. Millar, J. Christopher, and L. Kurbansik. Acridine araphanes: a new class of probe molecules for biological systems. *Science (Washington D. C.)* **205**:1277–1288 (1979).
25. Taylor, J. L., R. T. Mayer, and C. M. Himel. Conformers of acetylcholinesterase: a mechanism of allosteric control. *Mol. Pharmacol.* **45**:74–83 (1994).
26. Jahr, C. E., and C. F. Stevens. A quantitative description of NMDA receptor-channel kinetic behavior. *J. Neurosci.* **10**:1830–1837 (1990).
27. Cull-Candy, S. G., and M. M. Usowicz. Multiple conductance channels activated by excitatory amino acids in cerebellar neurons. *Nature (Lond.)* **325**:525–528 (1987).
28. Neher, E., and J. H. Steinbach. Local anaesthetics transiently block currents through single acetylcholine-receptor channels. *J. Physiol. (Lond.)* **277**:153–176 (1978).
29. Monyer, H., R. Sprengel, R. Schoepfer, A. Herb, M. Higuchi, H. Lomeli, N. Burnashev, B. Sakmann, and P. H. Seeburg. Heteromeric NMDA receptors: molecular and functional distinction of subtypes. *Science (Washington D. C.)* **256**:1217–1221 (1992).
30. Kutsuwada, T., K. Nobuko, H. Mori, K. Sakimura, E. Kushiya, K. Araki, H. Meguro, H. Masaki, T. Kumanishi, M. Arakawa, and M. Mishina. Molecular diversity of the NMDA receptor channel. *Nature (Lond.)* **358**:36–41 (1992).
31. Kleckner, N. N., and R. Dingledine. Regulation of hippocampal NMDA receptors by magnesium and glycine during development. *Mol. Brain Res.* **11**:151–159 (1991).
32. Miller, C. Competition for block of a Ca^{2+}-activated K^+ channel by charybdotoxin and tetraethlyammonium. *Neuron* **1**:1003–1006 (1988).
33. Reynolds, I. J., and R. J. Miller. Multiple sites for the regulation of the *N*-methyl-D-aspartate receptor. *Mol. Pharmacol.* **33**:581–584 (1988).
34. Woodhull, A. M. Ionic blockage of sodium channels in nerve. *J. Gen. Physiol.* **87**:687–708 (1973).

Send reprint requests to: Edson X. Albuquerque, Department of Pharmacology and Experimental Therapeutics, University of Maryland, School of Medicine, 655 W. Baltimore St., Baltimore, MD 21201.